Chinese Chemical Letters 34 (2023) 107632

Contents lists available at ScienceDirect

Chinese Chemical Letters

journal homepage: www.elsevier.com/locate/cclet

[5]Rotaxane, linear polymer and supramolecular organic framework constructed by *nor-seco*-cucurbit[10]uril-based ternary complexation

Pan-Qing Zhang[a,1], Qian Li[b,1], Ze-Kun Wang[b], Qing-Xuan Tang[a], Pei-Pei Liu[a], Wen-Hao Li[a], Guan-Yu Yang[a], Bo Yang[a,*], Da Ma[c,*], Zhan-Ting Li[b]

[a] College of Chemistry, Zhengzhou University, Zhengzhou 450001, China
[b] Department of Chemistry, Fudan University, Shanghai 200438, China
[c] School of Pharmaceutical and Materials Engineering, & Institute for Advanced Studies, Taizhou University, Jiaojiang 318000, China

ARTICLE INFO

Article history:
Received 20 March 2022
Revised 19 June 2022
Accepted 21 June 2022
Available online 25 June 2022

Keywords:
Rotaxane
Linear polymer
Supramolecular organic framework
nor-seco-Cucurbit[10]uril
Ternary complexation

ABSTRACT

Here we use *nor-seco*-cucurbit[10]uril (*ns*-CB[10]) based ternary complexation to construct [5]rotaxane, linear supramolecular dynamic rotaxane polymers and cubic 3D supramolecular organic framework. A [5]rotaxane is constructed by *ns*-CB[10], TMeCB[6] and short linear derivatives of 4,4′-bipyridinium (**M2**). *ns*-CB[10], CB[7] and long linear derivatives of 4,4′-bipyridinium (**M3**) self-assemble into a linear supramolecular dynamic rotaxane polymer. *ns*-CB[10] and tetracationic tetrahedral monomer self-assemble and form a three-dimensional supramolecular organic framework. The above results demonstrate that *ns*-CB[10]-based ternary complexation is a versatile platform to build various supramolecular systems.

There are ever-growing requirements for molecular structural complexity to achieve functions and applications [1,2]. Self-assembly is an essential process in nature, which plays a critical role in the construction of sophisticated supramolecular materials. Self-assembly is of great importance in chemistry, materials science and biology [3–6]. The advanced integrative self-assembly systems are capable of integrating different components into one complex system with precise control of the structure. This supramolecular strategy enhances the complexity and diversity of synthetic supramolecular architectures and realizes the implementation of complex functions [7–9]. Macrocyclic hosts, including crown ethers [10–12], cyclodextrins [13], calixarenes [14], cucurbiturils [15–17] and pillararenes [18–21], have emerged as important components for the construction of self-assembly systems and materials. These hosts have been widely used to fabricate supramolecular aggregates with tailor-made topology and functions.

Cucurbit[*n*]urils (CB[*n*]), a family of highly symmetrical pumpkin shaped macrocycle host molecules with rigid hydrophobic cavity, have tight and selective binding towards various guest molecules, have great applications [15–17]. In particular, CB[8] is capable of simultaneously binding two guests to form ternary complexes. This CB[8]-based ternary complexation has been used as a supramolecular "cross-linker" to construct supramolecular polymers, supramolecular organic frameworks and supramolecular materials [22–39]. A *nor-seco*-cucurbit[10]uril (*ns*-CB[10]) is a double cavity host molecule [40–47], which is able to form ternary complexes. We decide to use the *ns*-CB[10]-based ternary complexation to construct supramolecular structures of different dimensions. By applying *ns*-CB[10] and other CB[*n*] homologues, we are able to construct [5]rotaxane, linear supramolecular dynamic rotaxane polymers and cubic 3D supramolecular organic framework (SOF).

Self-assembled (*pseudo*)rotaxane and rotaxane-type polymers based on CB[*n*] host molecules have been widely used in various applications [48]. Disulfide bonds are common in biological systems, especially in proteins, and are important in dynamic covalent chemistry [49–52]. CB[6] could selectively encapsulate the sulfhydryl or disulfide part of the guest molecules and have certain inhibitory or protective effect [53]. We designed and synthesized linear compounds **M1**, **M2** and **M3** with sulfhydryl or disulfide moiety, to study its self-assembly with *ns*-CB[10], tetramethyl CB[6] (TMeCB[6]) and CB[7] towards the formation of [5]rotaxane and linear supramolecular dynamic rotaxane polymers (Fig. 1). Tetrahedral compound **T1** was synthesized to study its assembly with *ns*-CB[10] towards the formation of SOF (Fig. 1). Compound **G1** was used as a model guest to study the ternary complexation with *ns*-CB[10].

The binding between compound **M1** and TMeCB[6] was investigated. The crystal structure of the complex formed between **M1**

* Corresponding authors.
E-mail addresses: yb08220425@163.com (B. Yang), dama@fudan.edu.cn (D. Ma).
[1] These authors contributed equally to this work.

https://doi.org/10.1016/j.cclet.2022.06.055
1001-8417/

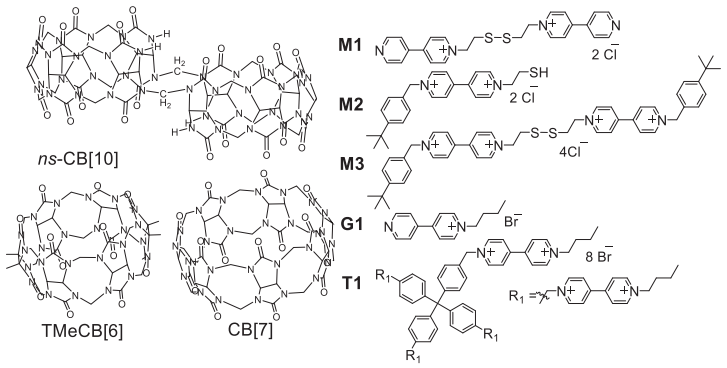

Fig. 1. Structures of **M1**, **M2**, **M3**, **G1**, **T1**, TMeCB[6], CB[7] and *ns*-CB[10].

and TMeCB[6] revealed a 1:1 binding stoichiometry and the S-S bond of **M1** was encapsulated in the cavity of the TMeCB[6] cavity (Fig. 2a). Combined with the stacking of bipyridine, a quadrilateral two-dimensional structure was formed, which was similar to structures reported in literature (Fig. 2b) [54]. The S-S bond of **M1** was encapsulated in TMeCB[6] was confirmed by ^{1}H NMR spectroscopy in D_2O. 1:1 binding stoichiometry was confirmed by absorption spectrum in solution (Figs. S1 and S2 in Supporting information). Due to the bulky *tert*–butyl benzene group, compound **M3** was unable to thread through the cavity of TMeCB[6]. Instead, compound **M3** binded to the carbonyl oxygen portal of TMeCB[6], which was confirmed by ^{1}H NMR spectroscopy and absorption spectrum (Figs. S3 and S4 in Supporting information). Disulfide bond was a dynamic covalent bond under weak alkalescent conditions. We discovered that disulfide bond was cleaved when growing single crystals with the solution of **M3**, TMeCB[6] and *ns*-CB[10] (**M3**:TMeCB[6]:*ns*-CB[10] = 1:1:1), which might be due to the residual alkaline from the synthesis of *ns*-CB[10] (Fig. 2c and Fig. S3). TMeCB[6] and *ns*-CB[10] encapsulated the sulfhydryl moiety and tert–butyl benzene moiety of the cleaved product **M2**, respectively. Due to the outer-surface interactions [17], a very regular arrangement structure was formed, *ns*-CB[10] and TMeCB[6] were showed hexagonal and rhomboid quadrilateral distribution, respectively (Fig. 2d). The complexation of compound **M2**, TMeCB[6] and *ns*-CB[10] (**M2**:TMeCB[6]:*ns*-CB[10] = 1:1:0.5) was studied by ^{1}H NMR spectroscopy (Fig. S5 in Supporting information). TMeCB[6] encapsulated sulfhydryl moiety and *ns*-CB[10] encapsulated *tert*–butyl benzene moiety to form a [5]rotaxane, which was in line with the crystal structure (Fig. 2c).

To extend the [5]rotaxane into supramolecular polymer, TMeCB[6] was replaced by CB[7], whose cavity was spacious enough to be threaded by *tert*–butyl benzene group. The self-assembly of compound **M1**, compound **M3,** *ns*-CB[10] and CB[7] was evaluated (Fig. 3). ^{1}H NMR and absorption spectra of **M1** and CB[7] showed similar observations as **M1**@TMeCB[6], the S-S bond of **M1** was encapsulated in the cavity of the CB[7] to form a complex with 1:1 binding stoichiometry (Figs. S6-S8 in Supporting

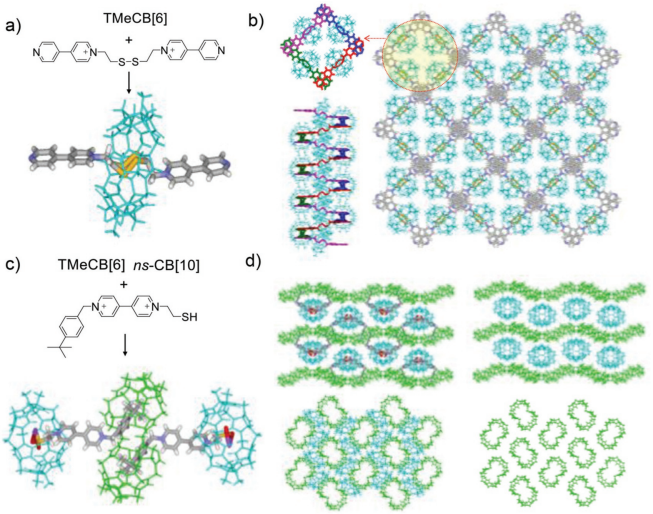

Fig. 2. Crystal structures of **M1**@TMeCB[6] (a, b) and **M2**@TMeCB[6]&*ns*-CB[10] (c, d).

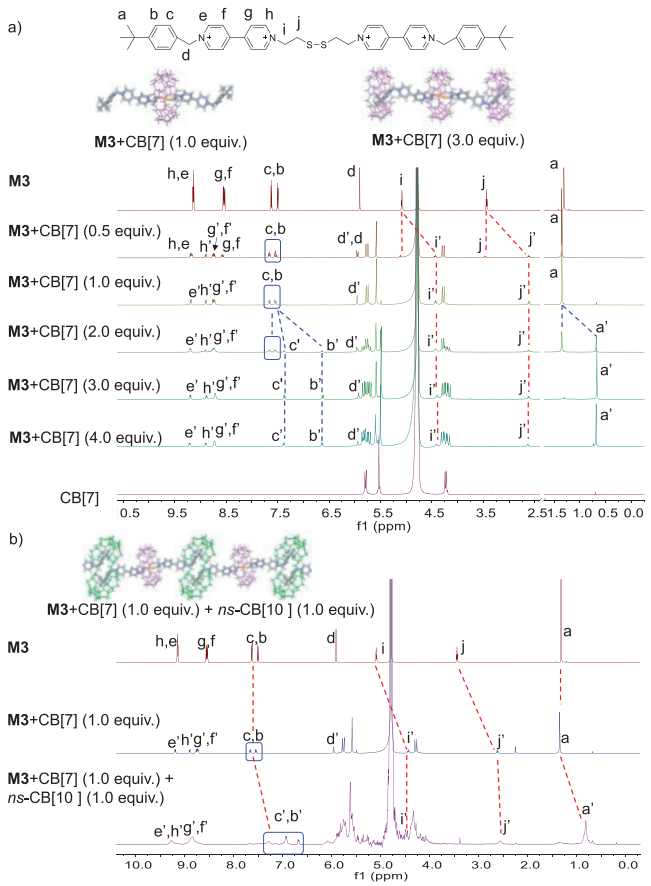

Fig. 3. (a) ^{1}H NMR spectra (400 MHz) of the mixture of **M3** (1.0 mmol/L) and CB[7] of various amount (0 to 4.0 equiv.) in D_2O at 25 °C. (b) ^{1}H NMR spectra (400 MHz) of free **M3**, **M3**+CB[7] (1.0 equiv.) and **M3** + CB[7] (1.0 equiv.) + *ns*-CB[10] (1.0 equiv.) in D_2O at 25 °C.

information). While for **M3** and CB[7], ^{1}H NMR spectroscopy revealed a formation of rotaxane or pseudorotaxane. When the binding stoichiometry of **M3** and CB[7] was 1:1, the S-S bond of **M3** was encapsulated by CB[7] (Fig. 3a) display upfield shifts ($\Delta\delta = -0.66$ and -0.84 for H_i and H_j, respectively). By contrast, when the binding stoichiometry was 1:3, a [4]rotaxane was formed (Fig. 3a). The 1:3 binding stoichiometry was confirmed by absorption spectrum in solution (Figs. S9 and S10 in Supporting information). In this [4]rotaxane, CB[7] encapsulated S-S bond and then *tert*–butyl benzene group ($\Delta\delta = -0.30$, -0.90 and -0.70 for H_c, H_b and H_a, respectively). We further increase the complexity by adding *ns*-CB[10] into the system [46]. Compound **M3**, CB[7] and *ns*-CB[10] were mixed in solution with a molar ratio of 1:1:1. ^{1}H NMR spectroscopy revealed that S-S bond was encapsulated in CB[7], and *tert*–butyl benzene was encapsulated in *ns*-CB[10], displayed upfield shifts ($\Delta\delta = -0.66$, -0.84, -0.73, -0.87 and -0.55 for H_i, H_j, H_c, H_b and H_a, respectively) (Fig. 3b). Comparing to the crystal structure of **M2**@TMeCB[6]&*ns*-CB[10], we believe **M3**, CB[7] and *ns*-CB[10] formed a linear supramolecular dynamic rotaxane polymers. Dynamic light scattering (DLS) experiments for the solution of **M3**, CB[7] and *ns*-CB[10] (1:1:1) ([**M3**] = 1.0 mmol/L, CB[7] = 1.0 mmol/L, *ns*-CB[10]=1.0 mmol/L) gave rise to a hydrodynamic diameter (D_H) of 531 nm, significantly larger than that for [4]rotaxane (18 nm, [**M3**] = 1.0 mmol/L, CB[7] = 3.0 mmol/L) (Fig. S11 in Supporting information). 2D diffusion-ordered NMR spectroscopy (DOSY) further confirmed the supramolecular polymers. The diffusion coefficient of **M3**/CB[7]/*ns*-CB[10] (1:1:1, 0.5 mmol/L) in water was 8.9×10^{-11} m^2/s, and based on the DOSY results, the molecular weight of the supramolecular polymer was calculated to be 4.3×10^4 Da, the result were similar to *nor-seco*-cucurbit[10]uril based linear supramolecular polymer by Xu *et al.* [46] (Fig. S12 in Supporting information). These observations indicated a *ns*-CB[10] based supramolecular dynamic rotaxane polymers formed.

Before *ns*-CB[10] was used to construct SOF, the binding between *ns*-CB[10] and compound **G1** was studied. The crystal structure for the complex of **G1** and *ns*-CB[10] revealed a 2:1 binding stoichiometry and the formation of [3]rotaxane. In the [3]rotaxane, the two butyl of **G1** were antiparallelly encapsulated in the two cavities of the *ns*-CB[10] (Fig. 4a), which was also confirmed in D_2O by ^{1}H NMR spectroscopy (Fig. S13 in Supporting information). Next, compound **T1** and *ns*-CB[10] was mixed to construct 3D SOF (*ns*-SOF-Bu) (Fig. 4b). ^{1}H NMR spectra showed that compound **T1** formed complex with *ns*-CB[10] with a 1:2 binding stoichiometry, which was confirmed by a maximum proton resonance upfield shift when 2.0 equivalent *ns*-CB[10] was added (Fig. S14 in Supporting information). DLS experiments for the solution of **T1** and *ns*-CB[10] (1:2) gave rise to a D_H ranging from 342 nm to 615 nm, depending on the concentration of the mixture ([**T1**] = 0.03–1.0 mmol/L), indicating the formation of nanostructures (Fig. 4c). The structural ordering of *ns*-SOF-Bu was investigated with synchrotron small-angle X-ray scattering (SAXS) and selected area electron diffraction (SAED). This scattering signal of *ns*-SOF-Bu corresponded to the simulated {001} and {111} spacing 2.48 nm and 1.83 nm of a modeled network (Figs. 4d and e), simulated on the basis of the crystal structure of the 2:1 complex of **G1** and *ns*-CB[10] and the interpenetrated crystal structure 1:2 complex of **T1** and CB[8] (SOF-Bu) [34]. According to the larger structural characteristics of *ns*-CB[10], the unit-cell parameters of modeled interpenetrated structure *ns*-Bu-SOF are slightly larger than crystal structure SOF-Bu, and the aperture of the cyclohexane-like pore of interpenetrated *ns*-Bu-SOF in modeled interpenetrated structure was measured to be 2.5 nm, larger than 2.1 nm of crystal structure of SOF-Bu [34]. The SAED pattern of different microcrystals of *ns*-SOF-Bu showed the {040} and {004} lattice spacings as being viewed from the [100] lattice direction (Figs. 5a-d). Elemental mapping analysis of the microcrystals

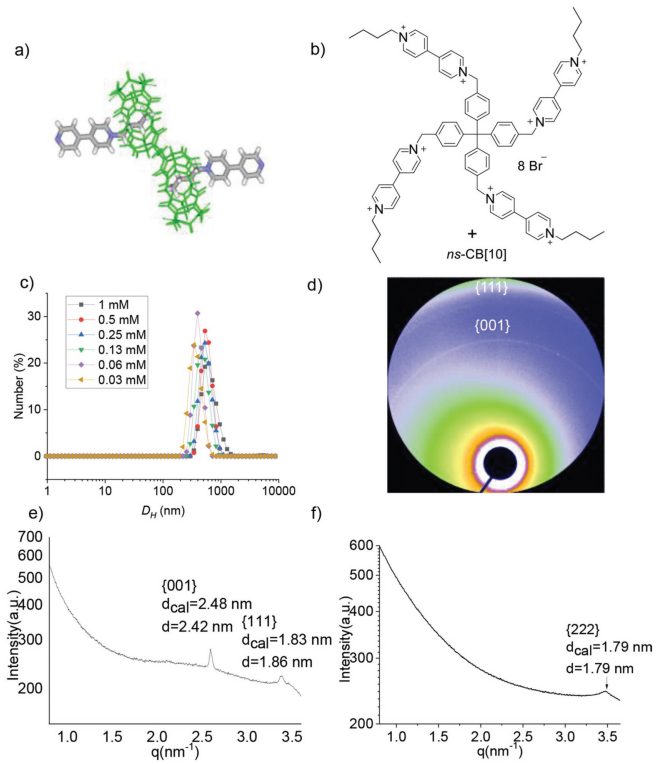

Fig. 4. (a) The crystal structure of [**G1**]$_2$@*ns*-CB[10]. (b) Compound structure of **T1.** (c) The hydrodynamic diameters of the aggregates of *ns*-SOF-Bu at different concentrations in water at 25 °C. (d) Solid-phase 2D SAXS image of *ns*-SOF-Bu. (e) Solid-phase SAXS profiles of *ns*-SOF-Bu. (f) Solution-phase profiles of *ns*-SOF-Bu.

confirmed the compositions of the C, N, O, Br elements (Fig. S15 in Supporting information). All the above observations showed a high regularity of *ns*-SOF-Bu in the solid state. The structural ordering of *ns*-SOF-Bu in solution was also confirmed by SAXS, the scattering signal corresponded to the simulated {222} spacing 1.79 nm of a modeled network (Fig. 4f). And referenced to literatures methods [34], to test if the *ns*-SOF-Bu formed non-interpenetrating pores in solution, dialysis experiments were carried out for two dyes acid red 27 and 4,4′,4″,4‴-porphyrin-5,10,15,20-tetrabenzoate (PTB, as sodium salt) using dialysis bags (MWCO: 1000 Da). The result showed that *ns*-SOF-Bu was able to completely retained the dyes from escaping ($\lesssim$1.0%) (Fig. S16 in Supporting information), indicating SOF was a porous structure in water. Therefore, a non-interpenetrated porous framework was formed in solution (Fig. 5f).

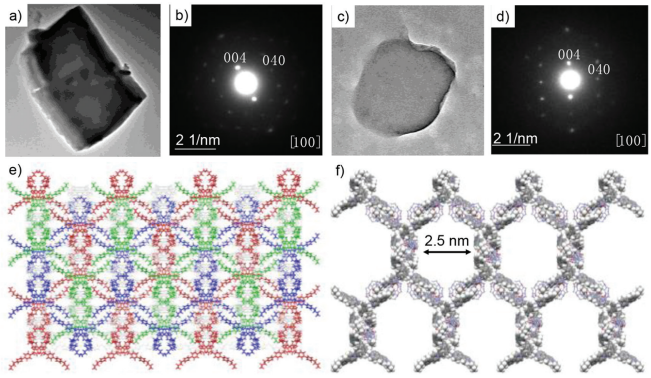

Fig. 5. (a, c) Microcrystals of *ns*-SOF-Bu as recorded by TEM, and (b, d) their SAED patterns which showed the reciprocal lattice observed for the [100] facet and foursquare order. (e) Model structure of *ns*-SOF-Bu in solid, and (f) model structure of *ns*-SOF-Bu in solution.

This solid of *ns*-SOF-Bu by evaporation was also used to adsorb acid red 27, the adsorption percentage was 40%, which may be rationalized by considering partial formation of the interpenetrated structures (Fig. S17 in Supporting information).

Diluting the solution of [5]rotaxane (**M2**/*ns*-CB[10]/TMeCB[6]), [4]rotaxane (**M3**/CB[7]), linear supramolecular dynamic rotaxane polymers (**M3**/CB[7]/*ns*-CB[10]), and *ns*-SOF-Bu (**T1**/*ns*-CB[10]) from 1.0 mmol/L to 0.05 mmol/L did not cause observable shifting of the signals in ^{1}H NMR in D_2O (Figs. S18-S21 in Supporting information). The ^{1}H NMR spectrum of the sample in D_2O did not exhibit any change after being placed at room temperature for more than 96 h (Figs. S18-S21). Both results confirmed the high stability of the new supramolecular framework in solution.

In summary, *ns*-CB[10]-based ternary complexation was used to construct rotaxanes, linear supramolecular polymers and 3D supramolecular organic frameworks. It demonstrated that *ns*-CB[10] could act as a supramolecular cross-linker to building finite molecular devices and infinite supramolecular materials. This discovery has a major implication for CB[*n*]-based crystal engineering and material assembly.

Declaration of competing interest

The authors declare that they have no known competing financial interests or personal relationships that could have appeared to influence the work reported in this paper.

Acknowledgments

We thank the supports from the National Natural Science Foundation of China (Nos. 21890732, 21890730 and 21921003). SAXS data were collected with beamline BL16B1 at Shanghai Synchrotron Radiation Facility.

Supplementary materials

Supplementary material associated with this article can be found, in the online version, at doi:10.1016/j.cclet.2022.06.055.

References

[1] G.M. Whitesides, J.P. Mathias, C.T. Seto, Science 254 (1991) 1312–1319.
[2] J.S. Siegel, Science 338 (2012) 752–753.
[3] H.V. Schröder, Y. Zhang, A.J. Link, Nat. Chem. 13 (2021) 850–857.
[4] H.T. Feng, J.W.Y. Lam, B.Z. Tang, Coord. Chem. Rev. 406 (2020) 213142.
[5] E. Winfree, F. Liu, L.A. Wenzler, et al., Nature 394 (1998) 539–544.
[6] J. Dong, Y. Pan, H. Wang, et al., Angew. Chem. Int. Ed. 59 (2020) 10151–10159.
[7] W. Jiang, A. Schäfer, P.C. Mohr, et al., J. Am. Chem. Soc. 132 (2010) 2309–2320.
[8] L. Wang, L. Cheng, G. Li, et al., J. Am. Chem. Soc. 142 (2020) 2051–2058.
[9] M.M. Safont-Sempere, G. Fernández, F. Würthner, Chem. Rev. 111 (2011) 5784–5814.
[10] C.J. Pedersen, Angew. Chem. Int. Ed. 27 (1988) 1021–1027.
[11] C.J. Pedersen, Science 241 (1988) 536–540.
[12] B. Zheng, F. Wang, S. Dong, et al., Chem. Soc. Rev. 41 (2012) 1621–1636.
[13] M. Miyauchi, A. Harada, J. Am. Chem. Soc. 126 (2004) 11418–11419.
[14] D.S. Guo, Y. Liu, Chem. Soc. Rev. 41 (2012) 5907–5921.
[15] S.J. Barrow, S. Kasera, M.J. Rowland, et al., Chem. Rev. 115 (2015) 12320–12406.
[16] X.L. Ni, X. Xiao, H. Cong, et al., Acc. Chem. Res. 47 (2014) 1386–1395.
[17] Y. Huang, R.H. Gao, M. Liu, et al., Angew. Chem. Int. Ed. 60 (2021) 15166–15191.
[18] Y. Liu, S. Jiang, W. Mao, et al., Chin. Chem. Lett. 33 (2022) 209–212.
[19] Z. Zhang, Y. Luo, J. Chen, et al., Angew. Chem. Int. Ed. 50 (2011) 1397–1401.
[20] S. Lan, S. Zhan, J. Ding, et al., J. Mater. Chem. A 5 (2017) 2514–2518.
[21] Y.P. Jiao, S. Lan, D. Ma, Chin. Chem. Lett. 32 (2021) 1025–1028.
[22] S. Jiang, W. Mao, D. Mao, et al., Chin. Chem. Lett. 33 (2022) 881–884.
[23] Y. Yang, H. Hu, L. Chen, et al., Mater. Chem. Front. 3 (2019) 806–811.
[24] X. Tang, Z. Huang, H. Chen, et al., Angew. Chem. Int. Ed. 57 (2018) 8545–8549.
[25] W. Xu, Q. Song, J.F. Xu, et al., ACS Appl. Mater. Interfaces 9 (2017) 11368–11372.
[26] R. Fang, H. Zhang, L. Yang, et al., J. Am. Chem. Soc. 138 (2016) 16372–16379.
[27] L. Yang, X. Tan, Z. Wang, et al., Chem. Rev. 115 (2015) 7196–7239.
[28] K.D. Zhang, J. Tian, D. Hanifi, et al., J. Am. Chem. Soc. 135 (2013) 17913–17918.
[29] J. Tian, T.Y. Zhou, S.C. Zhang, et al., Nat. Commun. 5 (2014) 5574.
[30] J. Tian, Z.Y. Xu, D.W. Zhang, et al., Nat. Commun. 7 (2016) 11580.
[31] Y. Li, Y. Dong, X. Miao, et al., Angew. Chem. Int. Ed. 57 (2018) 729–733.
[32] B. Yang, X.D. Zhang, J. Li, et al., CCS Chem. 1 (2019) 156–165.
[33] B. Yang, H. Wang, D.W. Zhang, et al., Chin. J. Chem. 38 (2020) 970–980.
[34] B. Yang, J.W. Zhang, S.B. Yu, et al., Sci. China Chem. 64 (2021) 1228–1234.
[35] B. Yang, S.B. Yu, P.Q. Zhang, et al., Angew. Chem. Int. Ed. 60 (2021) 26268–26275.
[36] J. Liu, Y. Lan, Z. Yu, et al., Acc. Chem. Res. 50 (2017) 208–217.
[37] J. Zhang, R.J. Coulston, S.T. Jones, et al., Science 335 (2012) 690–694.
[38] Q. Li, J.D. Sun, B. Yang, et al., Chin. Chem. Lett. 33 (2022) 1988–1992.
[39] Y.P. Wu, M. Yan, Z.Z. Gao, et al., Chin. Chem. Lett. 30 (2019) 1383–1386.
[40] W.H. Huang, S. Liu, P.Y. Zavalij, et al., J. Am. Chem. Soc. 128 (2006) 14744–14745.
[41] E.A. Appel, J.d. Barrio, J. Dyson, et al., Chem. Sci. 3 (2012) 2278–2281.
[42] M.I. El-Barghouthi, H.M. Abdel-Halim, F.J. Haj-Ibrahim, et al., J. Incl. Phenom. Macrocycl. Chem. 82 (2015) 323–333.
[43] X. Zhang, W. Wu, Z. Tao, et al., Beilstein. J. Org. Chem. 15 (2019) 1705–1711.
[44] K.M. Park, J.H. Roh, G. Sung, et al., Chem. Asian J. 12 (2017) 1461–1464.
[45] R. Nally, L. Isaacs, Tetrahedron 65 (2009) 7249–7258.
[46] Y. Yang, X.L. Ni, J.F. Xu, et al., Chem. Commun. 55 (2019) 13836–13839.
[47] J.B. Wittenberg, M.G. Costales, P.Y. Zavalij, et al., Chem. Commun. 47 (2011) 9420–9422.
[48] Q.Z. Han, Y. Li, J. Incl. Phenom. Macrocycl. Chem. 92 (2018) 1–101.
[49] S. Otto, R.L.E. Furlan, J.K.M. Sanders, Science 297 (2002) 590–593.
[50] B. Brisig, Chem. Int. Ed. 42 (2010) 1270–1273.
[51] J.M.A. Carnall, C.A. Waudby, A.M. Belenguer, et al., Science 327 (2010) 1502–1506.
[52] B. Balakrishna, A. Menon, K. Cao, et al., Angew. Chem. Int. Ed. 59 (2020) 18774–18785.
[53] L.S. Berbeci, W. Wang, A.E. Kaifer, Org. Lett. 10 (2008) 3721–3724.
[54] J. Li, Y. Zhao, Y. Dong, et al., CrystEngComm 18 (2016) 7929–7933.